

INVESTIGATIONS INTO NON-LINEAR BEAM DYNAMICS IN ELECTROSTATIC STORAGE RINGS

D. Newton, C.P. Welsch, Cockcroft Institute and the University of Liverpool, UK
 O.I. Papash, O. Gorda, Max Planck Institute for Nuclear Physics, Heidelberg, Germany

Abstract

Electrostatic (ES) storage rings provide a cost-effective solution to the problem of confining low energy ($\beta \ll 1$) charged particles and ions, whilst controlling the beam properties, for use in multi-pass experiments. However, compared to magnetic storage rings, the beam dynamics calculations for an ES ring show subtle differences, especially in the coupling of the longitudinal and transverse velocities and in the focusing properties of bending element fringe fields. Using the nominal design for an existing ES ring, realistic trajectories (including fringe fields and non-linear field components) have been calculated and a comparison is made with linear lattice simulations. The effect of the non-linear field components on the beam parameters is discussed.

INTRODUCTION

In the future Facility for Low-energy Anti-proton and Ion Research (FLAIR) at FAIR, the Ultra-low energy electrostatic Storage Ring (USR) will provide cooled beams of anti-protons down to energies of 20 keV. The large variety of envisaged experiments requires a very flexible ring lattice to provide beams with variable cross sections, shapes and time structures, ranging from ultra-short pulses to a coasting beam. Although a few electrostatic storage rings are in operation around the world, little detailed investigation into the beam dynamics of these machines has been carried out. In this paper we present preliminary results of an investigation into the impact of non-linear effects on anti-proton trajectories. A nominal lattice based on the

ELISA ring [1], for which some diagnostic measurements exist, was used throughout the paper.

CODE BENCHMARKING

Charged particle dynamics in electro-static fields differ from those in magnetic fields in that the particle energy is a function of the particle position in the ES element. At relativistic energies the change in the particle velocity is negligible but for the energies under consideration at the USR where $\beta \ll 1$, the change in kinetic energy may be large enough to invalidate the paraxial approximation of constant velocity that many lattice codes make. To investigate this situation a numerical tracking code was written in C++ which uses the ODE solver CVODE (part of the SUNDIALS suite [2]) to numerically solve the equations of motion. For absolute benchmarking, particle tracking was carried out in a spherical ES deflector (ESD), with a potential, in spherical coordinates of $\phi \propto r^{-1}$ [3]. This potential is the same as the gravitational potential and so Kepler orbits can be used to give an analytical solution to the particle motion. Anti-protons with kinetic energy, $E_K = 22$ keV were tracked through a 360° spherical deflector (bend radius=0.25 m), with CVODE and COSY [4], and compared with the analytical Kepler orbit. The displacement from the reference orbit is shown in Fig. 1. All three trajectories agree reasonably well, though it can be seen in the inset plot that the assumption of constant velocity in COSY gives a slight deviation from the CVODE and Kepler trajectories. A similar difference was found between the trajectories in cylindrical ESDs ($\phi \propto \ln(1/r)$) and to a lesser extent in ES quadrupole elements. These small discrepancies may be important in multi-turn simulations to calculate the beam lifetime.

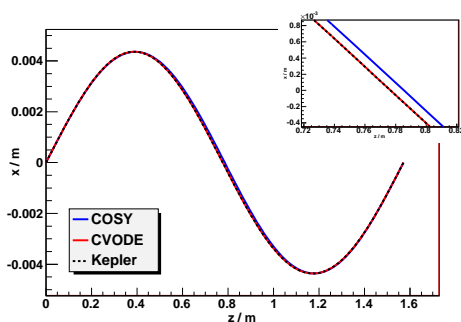


Figure 1: Anti-proton trajectories in a spherical ESD. COSY and CVODE results are compared with an analytic Kepler trajectory. Inset: A close up highlighting the discrepancy with the COSY trajectory.

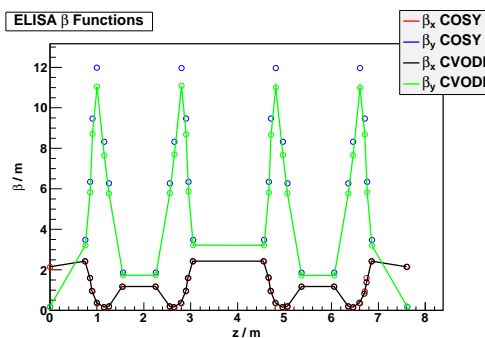


Figure 2: ELISA beta functions calculated with COSY and CVODE.

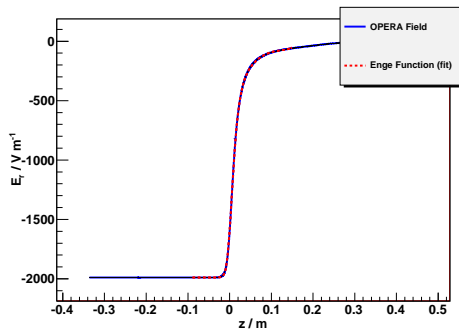


Figure 3: Cylindrical ESD fringe fields, fitted with a six parameter Enge function.

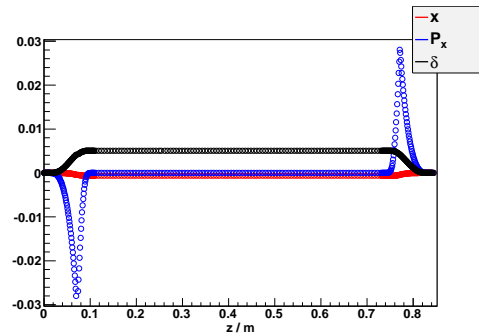


Figure 4: Numerical tracking through a cylindrical ESD fringe field (canonical coordinates).

LATTICE COMPARISONS

An ES lattice based on the ELISA lattice was chosen to assess the different tracking codes. This lattice has race-track design composed of two cells, with each cell having the configuration:

$$QF \ QD \ ESD_{cyl} \ ESD_{cyl} \ ESD_{cyl} \ QD \ QF$$

The quadrupole settings were initially fitted in COSY to find a stable orbit, then the trajectories and lattice functions were calculated in both COSY and CVOICE. In the horizontal transverse direction, the phase space ellipses compare well, with a similar phase advance: $Q_x = 2.8333$ (2.8341 ± 0.0001) in the case of COSY (CVOICE). Comparing the phase space ellipse in the vertical direction, COSY shows a larger momentum excursion than CVOICE, with similar tunes: $Q_y = 1.83$ (1.815 ± 0.001) in the case of COSY (CVOICE). The linear beta functions are shown in Fig. 2. The results are similar for CVOICE and COSY, though in the vertical direction, COSY gives a slightly higher value of β_y at the quadrupole locations.

ESD FRINGE FIELDS

The ELISA lattice discussed above has been modeled in the finite element solver, OPERA [5], to give a realistic model of the fringe fields and their affect on the particle trajectories. Figure 3 shows the OPERA fringe fields on the reference orbit for the cylindrical ESD, with a six parameter fitted Enge function.

Three methods were used to incorporate the fringe fields into lattice codes:

- The OPERA fringe field was modeled with an Enge function and implemented in CVOICE as a numerical extension to the ESD,
- The Enge function was used to calculate a fringe kick matrix in COSY,
- A multipole analysis was performed by taking a Fourier transform of the fringe field at a radius of 14 mm. The multiple components, to tenth order, were

used to generate a multipole element in MADX with linear matrices replacing the ES elements.

Trajectory Changes in the Fringe Field

Using the fitted Enge function, a realistic fringe field was incorporated into the CVOICE model with a scalar potential, $\phi \propto F_{ENGE}(\theta) \ln(1/r)$. This potential gives a radial electric field which follows the Enge function, but also leads to an azimuthal electric field, which accelerates the particle from zero potential outside the ESD to its final potential within the body of the ESD. Figure 4 shows the dynamical variables x , P_x and δ (where δ is the kinetic energy deviation from the reference particle). This plot shows that as the anti-proton enters the fringe field, it receives a kick in its horizontal momentum, which causes a change in x (relative to a reference particle, and a corresponding change in the kinetic energy (the ESD is modeled such that the zero potential lies on $x=0$). The kick in energy, momentum and position are useful in calculating the physical ESD parameters needed to give the required effective bending radius.

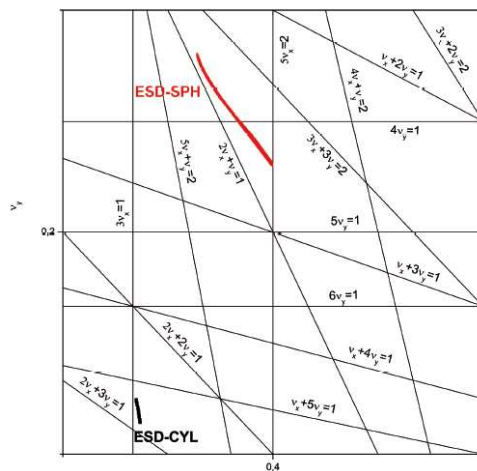


Figure 5: The amplitude dependent tuneshift for cylindrical and spherical ESDs in the ELISA lattice.

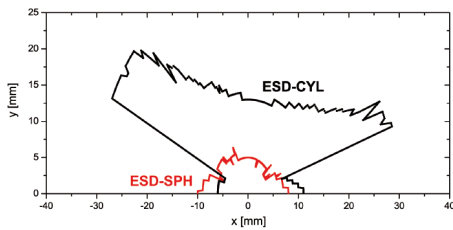


Figure 6: ELISA dynamic aperture with cylindrical and spherical ESDs.

Tuneshift and Dynamic Aperture

A multipole element, with parameters taken from a Fourier transform of the OPERA fringe field, was implemented in MADX to investigate the amplitude dependent tuneshift and the dynamic aperture. In this section the effects of both cylindrical and spherical ESDs were considered. Because of the inherent non-linearity of spherical and cylindrical ESDs, the motion of particles with large amplitudes is of particular interest.

To demonstrate how the tune spread can influence the nonlinear particle motion, the tune spread curves are plotted on a resonance diagram (Fig. 5). The tune spread for spherical ESDs is much larger than for cylindrical ESDs and crosses two resonances of fourth and fifth order. For the given working point, both curves are relatively close to third order resonances and so the stability of particle motion could be influenced by the ESD sextupole component.

The dynamic aperture of the ELISA lattice was calculated for spherical and cylindrical ESDs to compare the stability limit for these two cases. Particles with randomly assigned initial coordinates were tracked over 5000 turns. Surviving particles were assumed to lie within the dynamic aperture. The dynamic aperture of the lattice is shown in Fig. 6. Particles with high amplitude vertical betatron oscillations are more stable in the case when cylindrical deflectors are used.

STABILITY PLOTS

The option to include fringe fields is available in COSY, where the coefficients of the Enge function are given as a parameter, and the fringe field is modeled as a kick matrix of zero length.

Stability plots for magnetic lattices have a familiar ‘neck-tie’ appearance, showing regions of stability, where the trace of the linear 2x2 matrix (in the horizontal and vertical directions) is less than two: $|Tr(M)| \leq 2$. In these plots the quadrupoles supply the strong focusing and the weak focusing of the dipoles is negligible. This leads to a symmetry between the focusing and defocusing quadrupole strengths, $k_F l$ and $k_D l$, such that stability in one plane implies stability in the other plane. They are generally plotted in F and D space, where $F = (k_F l)^2$ and $D = (-k_D l)^2$. ESD lattices give very different stability plots. Cylindrical ESDs have a radial field that falls off as $1/r$, which gives

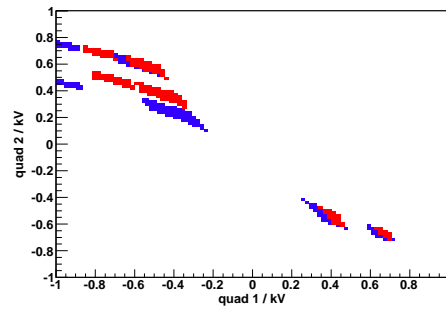


Figure 7: A scan of the ELISA quadrupole voltage parameter space showing regions of stability in both the horizontal and vertical transverse directions. Red: No Fringe Fields. Blue: With fringe fields.

focusing in the horizontal (x) direction and acts as a drift space in the vertical (y) direction. The presence of the ESD therefore breaks the symmetry between the focusing and defocusing quadrupoles, and means a region of stability in one plane will not necessarily coincide with a region of stability in the other plane. To investigate the stable regions in the ELISA lattice, a scan of the parameter space over the quadrupole strengths was made in COSY and the trace of the linear matrix was plotted at each point. The presence of fringe fields has a significant affect on the region of stability as can be seen in Fig. 7, where only regions that are stable in both transverse directions are plotted.

SUMMARY

Preliminary results have been presented into an investigation of the dynamics of electro-static rings at ultra-low energies. Work is ongoing to benchmark the different methods of describing the fringe field components and investigate the inherent non-linear behavior of electro-static bending elements, with the aim of optimising the nominal lattice design of the USR at FLAIR.

ACKNOWLEDGMENTS

This work is supported by the EU under contract PITN-GA-2008-215080 and HGF/GSI under VH-NG-328 and the Science and Technology Facilities Council, UK.

REFERENCES

- [1] Søren Papa Møller, ‘ELISA, an Electro-static Storage Ring for atomic physics’, NIM A 297 (1997).
- [2] SUNDIALS, <https://computation.llnl.gov/casc/sundials/main.html>.
- [3] H. Wollnik, ‘The Optics of Charged Particles’, Academic Press Inc., 1987.
- [4] K. Makino and M. Betz, ‘Cosy Infinity’, NIM A, 427 (1999).
- [5] OPERA, <http://www.cobham.com/about-cobham/aerospace-and-security/about-us/antenna-systems/kidlington/opera-14.aspx>.